Reassessment of the intrinsic carrier density temperature dependence in crystalline silicon

Romain Couderc,[1,2,a)] Mohamed Amara,[2] and Mustapha Lemiti[1]
[1]*Université de Lyon, Institut de Nanotechnologies INL-UMR5270, CNRS, INSA de Lyon, Villeurbanne F-69621, France*
[2]*Université de Lyon, Centre de thermique de Lyon CETHIL-UMR5008, CNRS, INSA de Lyon, Villeurbanne F-69621, France*

(Received 13 December 2013; accepted 24 February 2014; published online 6 March 2014; publisher error corrected 24 March 2014)

The intrinsic carrier density n_i of crystalline silicon is an essential parameter for the simulation of electrical and thermal behavior of silicon devices. At 300 K, a value of $n_i = 9.65 \times 10^9\,\mathrm{cm}^{-3}$ has been determined by extensive experimental studies. However, the temperature dependence of this parameter remains to be verified. In this work, we propose a new expression $n_i = 1.541 \times 10^{15} T^{1.712} \exp(-E_g^0/(2kT))$ thanks to an updated fit of experimental data. Polynomial fits of $(m_{dc}^*/m_0)^{\frac{3}{2}}$ and $(m_{dv}^*/m_0)^{\frac{3}{2}}$ are also proposed to model N_C and N_V. © *2014 AIP Publishing LLC*. [http://dx.doi.org/10.1063/1.4867776]

I. INTRODUCTION

One of the major parameters influencing the electrical and thermal behavior of a silicon device is the intrinsic carrier density n_i.[1] An accurate description of n_i in crystalline silicon as a function of the temperature is therefore of primary interest for simulations of silicon devices.

The accepted value of n_i at 300 K has been revised several times since the first estimates were made in the 1960 s. First, Green[2] adjusted the value from $n_i = 1.45 \times 10^{10}\,\mathrm{cm}^{-3}$ to $n_i = 1.08 \times 10^{10}\,\mathrm{cm}^{-3}$ following a critical investigation on former resistivity measurements. A few years after this first correction, Sproul[3,4] made a further refinement by means of experiments involving specially designed solar cells to determine $n_i = 1.00 \times 10^{10}\,\mathrm{cm}^{-3}$. Shortly afterwards, Misiakos[5] published another value, $n_i = 9.7 \times 10^9\,\mathrm{cm}^{-3}$, thanks to capacitance measurements of a pin diode biased under high injection. However, a literature review suggests that the commonly used value remains that provided by Sproul.

Recently, Altermatt[6] corrected the Sproul's value by taking into account bandgap narrowing (BGN) which allowed the two contemporary values of n_i to be brought to agreement. The recommended value at 300 K is currently given by Altermatt,[6] $n_i = 9.65 \times 10^9\,\mathrm{cm}^{-3}$, based on his work and the consistency found with Misiakos' previous measurement as mentioned by Altermatt in his conclusions. Altermatt suggested a corrected value of n_i taking into account BGN at 300 K but did not propose an expression for its temperature dependence. The most commonly used expressions of n_i as a function of temperature are those provided by the authors cited above. Significant discrepancies are observed between these, which thus impact upon the studies that utilize them.

The purpose of this paper is to reassess the temperature dependence of n_i by taking BGN into account. First, a theoretical review is presented. Second, the various bandgap models are considered and the most precise one chosen for use in the present work. Third, the correction of Sproul's data taking into account BGN is detailed. Finally, polynomial fits of the density of states (DOS) effective masses m_{dc}^* and m_{dv}^* are proposed to model the effective DOS N_C and N_V in the conduction band and in the valence band, respectively.

II. THEORY

Extensive studies have been undertaken to evaluate n_i; a critical analysis is necessary in order to make a good hypothesis and reevaluate the temperature dependence of n_i. The temperature dependence of n_i can be deduced by inspection of the following equation:

$$n_i^2 = N_C(T) N_V(T) \exp\left(\frac{-E_g^0(T)}{kT}\right), \tag{1}$$

where E_g^0 is the intrinsic bandgap of the semiconductor, k is the Boltzmann constant and T is the temperature. N_C and N_V are defined as follows:[8]

$$N_C = 2\left(\frac{2\pi m_{dc}^* kT}{h^2}\right)^{\frac{3}{2}}, \tag{2}$$

$$N_V = 2\left(\frac{2\pi m_{dv}^* kT}{h^2}\right)^{\frac{3}{2}}, \tag{3}$$

where h is the Planck constant. Using the recommended values[9] of the physical constants gives

$$N_C = 4.83 \times 10^{15} \left(\frac{m_{dc}^*}{m_0}\right)^{\frac{3}{2}} T^{\frac{3}{2}}(\mathrm{cm}^{-3}), \tag{4}$$

$$N_V = 4.83 \times 10^{15} \left(\frac{m_{dv}^*}{m_0}\right)^{\frac{3}{2}} T^{\frac{3}{2}}(\mathrm{cm}^{-3}), \tag{5}$$

where m_0 is the electron rest mass. Considering the silicon energy band diagram in the first Brillouin zone, m_{dc}^* and m_{dv}^* are given by

a)Electronic mail: romain.couderc@insa-lyon.fr

$$m_{dc}^* = 6^{\frac{2}{3}}\left(m_t^{*2} m_l^*\right)^{\frac{1}{3}}, \tag{6}$$

$$m_{dv}^* = \left(m_{lh}^{*\frac{3}{2}} + m_{hh}^{*\frac{3}{2}} + \left(m_{so}^* \exp\left(\frac{-\Delta}{kT}\right)\right)^{\frac{3}{2}}\right)^{\frac{2}{3}}, \tag{7}$$

where m_t^* is the transverse effective mass, m_l^* is the longitudinal effective mass, m_{lh}^* is the light hole band effective mass, m_{hh}^* is the heavy hole band effective mass, m_{so}^* is the split-off hole band effective mass, and Δ is the energy between the split-off band and the heavy and light hole bands. Experimental measurements of the effective masses are only possible at a temperature close to absolute zero because the cyclotron resonance observation requires a high carrier mobility.[10] Hence, all the existing models of n_i, experimental or theoretical, are usually expressed in the following form:

$$n_i = AT^B \exp\left(\frac{-C}{T}\right). \tag{8}$$

It is clear from Eq. (1) that n_i is directly linked to E_g^0. Section III addresses the choice of model to estimate E_g^0. Existing models of $n_i(T)$ and the correction of $n_i(T)$ due to BGN will be discussed in a subsequent section.

III. TEMPERATURE DEPENDENCE OF n_i

A. Bandgap models and implications for n_i

Three models of E_g^0 are predominantly in use, all of which are based on the experimental results of Bludau *et al.*[11] and Macfarlane *et al.*[12] Each model proposes a different fit of these data based on different hypotheses. The temperature dependence of these models is shown in Fig. 1. Thurmond[13] and Alex[14] based their fit on Varshni's hypothesis[15] of the form of Eq. (9), whereas Pässler[16] suggested an expression of the form of Eq. (10). The parameters for Thurmond, Alex, and Pässler models are listed in Table I.

$$E_g^0(T) = E_g^0(0) - \frac{\alpha T^2}{T+\beta}, \tag{9}$$

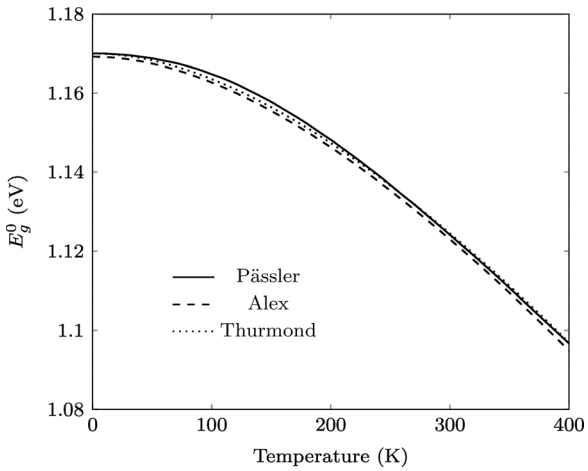

FIG. 1. Compilation of bandgap models versus temperature.

TABLE I. Parameters for Thurmond's, Alex's, and Pässler's model of E_g^0.

	Thurmond	Alex	Pässler
$E_g^0(0)$ (eV)	1.17	1.1692	1.17
α (eV K^{-1})	4.73×10^{-4}	4.9×10^{-4}	3.23×10^{-4}
β (K)	636	655	…
Θ (K)	…	…	446
Δ	…	…	0.51
γ	…	…	$\frac{1-3\Delta^2}{\exp(\Theta/T)-1}$
χ	…	…	$\frac{2T}{\Theta}$

$$E_g^0(T) = E_g^0(0) - \alpha\Theta\left[\gamma + \frac{3\Delta^2}{2}\left(1 + \frac{\pi^2}{3(1+\Delta^2)}\chi^2 + \frac{3\Delta^2-1}{4}\chi^3 + \frac{8}{3}\chi^4 + \chi^6\right)^{\frac{1}{6}} - 1\right]. \tag{10}$$

Though the discrepancies between the models are low, the implications on values of n_i are not. In order to study the consequences on the values of n_i, we defined in Eq. (11) a ratio between two expressions of n_i from the same model defined with two different models of E_g^0, subscripted x and y. This ratio is independent of the model of n_i and only sensitive to models of E_g^0

$$\frac{n_{i,x}}{n_{i,y}} = \exp\left(\frac{E_{g,y}^0 - E_{g,x}^0}{2kT}\right). \tag{11}$$

In Fig. 2, the temperature variation of the ratio between each model and Pässler's model is presented. It illustrates the non-negligible modification of n_i at low temperatures. The choice of model for E_g^0, therefore, has an impact on behavior as a function of temperature.

The higher precision of Pässler's model is demonstrated by the intrinsic unrealistic physical regime of extremely large dispersion implied by Varshni's model, which has not been observed in experiments.[17] For high temperature, $E_g^0(T)$ tends to a linear asymptote given by $E_{lim}(0) - \alpha T$, where α is the slope of the linear asymptote at high temperatures and

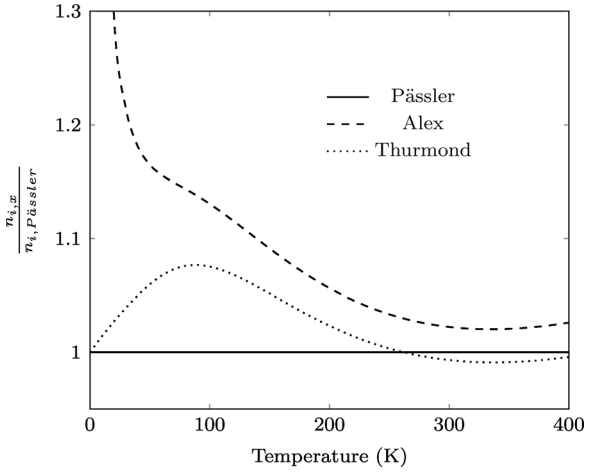

FIG. 2. $\frac{n_{i,x}}{n_{i,Pässler}}$, the ratio between n_i calculated with $E_{g,x}^0$ and n_i calculated with $E_{g,Pässler}^0$, as a function of temperature.

$E_{lim}(0)$ is the intercept of the asymptote at 0 K. The renormalization energy is defined as $E_{lim}(0) - E_g^0(0)$ and is equal to $\alpha\Theta/2$ for Pässler's model and $\alpha\beta$ for Varshni's model. The Alex's and Thurmond's α parameter and their renormalization energy are clearly overestimated compared to Pässler's parameters. Hence, for the sake of accuracy, $E_{g,Pässler}^0$ will be used hereafter.

B. Existing models of n_i and correction from BGN

The models from Hensel,[18] Madarasz,[19] and Humphreys[20] are theoretical models based on $k \cdot p$ perturbation theory.[22] The models from Green,[2] Sproul,[3,4] Misiakos[5] are semi-empirical models obtained from different measurements as detailed in the Introduction. Table II lists coefficients A, B, and C of Eq. (8) for the selected models and their temperature range of validity.

In this section, we seek to convince the reader that the current expressions of $n_i(T)$ from semi-empirical models are inadequate for modeling silicon devices at temperatures away from room temperature and demonstrate the necessity of a reassessment of the expression of $n_i(T)$.

Regarding only the data and not the expression of $n_i(T)$, Green's data cannot provide an accurate temperature dependence of n_i because of the uncertainty associated with the use of a generic model for the carriers mobilities instead of real measurements of the samples. Measurements by Sproul and Misiakos are sufficiently precise but their interpretation can be improved.

In his second paper, Sproul noted a good correlation between his values of n_i and the Hensel model in the temperature range 200 K to 375 K but not at lower temperatures. Based on this observation, Sproul did not trust his low temperature values of n_i and proposed an expression of $n_i(T)$ of the form of Eq. (8) (with $C = E_g^0(T)/(2k)$) based on the effective masses values of Hensel and E_g^0 based on Bludau's work.[11]

Indeed, the uncertainties on experimental estimates of n_i increase towards lower temperatures. Thus, it is interesting to compare these low temperature experimental values of n_i to the theoretical ones based on a knowledge of effective masses.[18–20] and very precise experimental values of the effective masses at temperature close to absolute zero.[18,21] Hence at low temperatures, the uncertainties of the theoretical values are lower than the uncertainties of the experimental values as mentioned by Sproul.[4]

TABLE II. Coefficients of Eq. (8) from different models and their temperature range of validity.

	A ($\times 10^{14}$)	B	C	T_{min} (K)	T_{max} (K)
Hensel	15.0	1.722	$\frac{E_g^0(T)}{2k}$	…	…
Humphreys	14.0	1.762	$\frac{E_g^0(T)}{2k}$	…	…
Madarasz	13.7	1.751	$\frac{E_g^0(T)}{2k}$	…	…
Green	16.8	1.715	$\frac{E_g^0(T)}{2k}$	200	500
Sproul (1991)	10.2	2	6880	275	375
Sproul (1993)	16.4	1.706	$\frac{E_g^0(T)}{2k}$	77	300
Misiakos	0.27	2.54	6726	78	340
This paper	15.41	1.712	$\frac{E_g^0(T)}{2k}$	77	375

Although this approach is valid, Sproul ignored BGN because available models at that time indicated no effect of BGN for the wafers used in the experiment. These models have subsequently been superseded by Schenk model,[7] which indicates a slight BGN for these wafers. Thus, Sproul did not measure the intrinsic carrier density n_i but rather the effective intrinsic carrier density $n_{i,eff}$. Hence, Sproul's values of n_i need to be reinterpreted to take into account BGN via Eq. (12), where ΔE_g is the BGN from Schenk's model

$$n_{i,eff} = n_i \exp\left(\frac{\Delta E_g}{2kT}\right) = n_i \gamma_{BGN}. \tag{12}$$

In the experiment setup used by Sproul,[3,4] the values of n_i are obtained thanks to Eq. (13)

$$n_i = \sqrt{\left(\frac{WN_A^-(I_{01} - I_{0e})}{1.025AqD_n\omega\coth\omega}\right)}, \tag{13}$$

where W is the quasi-neutral width of the wafer, N_A^- is the ionized dopant density, I_{01} is the saturation current, I_{0e} is the emitter saturation current, A is the cell area, D_n is the minority carrier electron diffusion constant, and ω is the ratio between the quasi-neutral width W and the minority carrier electron diffusion length L_n.

Sproul's data and the correction obtained using Schenk's model of BGN are summarized in Table III. The corrections are applied for the measurements of 10 Ω cm wafers from Sproul's papers. Wafers with a resistivity lower than 2 Ω cm were not considered because they are not suitable for extraction as discussed by Altermatt.[6] The calculations are not developed on the other wafers because they follow the exact same trend as the 10 Ω cm wafers. The wafers are 284 μm thick, and the area of the samples used to determine n_i are 4 cm^2.

In Table III, it is evident that the low temperature values from Sproul suffer the significant modification as a result of BGN. The corrected data, the Misiakos' data, and their fit of the form of Eq. (8) with $C = E_g^0(T)/(2k)$ are represented in Fig. 3. The expressions of $n_i(T)$ obtained are

$$n_{i,Misiakos} = 1.821 \times 10^{15} T^{1.699} \exp\left(\frac{-E_g^0}{2kT}\right), \tag{14}$$

$$n_{i,Sproul} = 1.541 \times 10^{15} T^{1.712} \exp\left(\frac{-E_g^0}{2kT}\right). \tag{15}$$

In our opinion, the expression obtained from Misiakos' data seems less pertinent because the value at 300 K is 1.06×10^{10} cm^{-3}, whereas the expression from Sproul's data gives 9.68×10^9 cm^{-3}, which is more consistent with the experimental value at 300 K obtained by the two studies. The Misiakos' data also agree less well with the theoretical models at low temperatures and exhibit a greater degree of scattering than Sproul's data. Furthermore, Misiakos' values of n_i at a temperature greater than 200 K are also fitting Eq. (15) as can be seen in Fig. 3.

TABLE III. Sproul's data corrected considering BGN.

T (K)	I_{01} (A)	I_{0e} (A)	N_A^- (cm^{-3})	D_n (cm^2/s)	$\omega\coth\omega$	n_i (cm^{-3})	γ_{BGN}	$n_{i,corrected}$ (cm^{-3})
77.4	3.38×10^{-69}	8.91×10^{-70}	8.1×10^{14}	88.1	1.018	3.12×10^{-20}	1.452	2.59×10^{-20}
110.6	2.11×10^{-51}	2.23×10^{-52}	1.16×10^{15}	84.0	1.011	3.34×10^{-11}	1.339	2.89×10^{-11}
125.9	2.30×10^{-39}	1.31×10^{-40}	1.27×10^{15}	79.4	1.007	3.86×10^{-5}	1.247	3.46×10^{-5}
151.2	2.84×10^{-31}	1.05×10^{-32}	1.30×10^{15}	71.7	1.006	4.62×10^{-1}	1.186	4.24×10^{-1}
200.3	2.65×10^{-21}	6.25×10^{-23}	1.31×10^{15}	56.0	1.004	5.11×10^{4}	1.120	4.82×10^{4}
250.3	4.17×10^{-15}	8.27×10^{-17}	1.32×10^{15}	43.0	1.003	7.35×10^{7}	1.085	7.06×10^{7}
275	7.52×10^{-13}	3.40×10^{-15}	1.35×10^{15}	38.8	1.003	1.06×10^{9}	1.074	1.02×10^{9}
275.3	7.92×10^{-13}	1.50×10^{-14}	1.32×10^{15}	38.5	1.003	1.07×10^{9}	1.073	1.03×10^{9}
300	5.94×10^{-11}	1.12×10^{-12}	1.32×10^{15}	34.7	1.003	9.78×10^{9}	1.064	9.48×10^{9}
300	5.90×10^{-11}	2.80×10^{-13}	1.35×10^{15}	34.6	1.003	9.94×10^{9}	1.065	9.63×10^{9}
325	2.56×10^{-9}	1.20×10^{-11}	1.35×10^{15}	31.1	1.003	6.90×10^{10}	1.058	6.71×10^{10}
350	6.40×10^{-8}	3.00×10^{-10}	1.35×10^{15}	28.2	1.003	3.63×10^{11}	1.051	3.54×10^{11}
375	1.08×10^{-6}	4.80×10^{-9}	1.35×10^{15}	25.8	1.003	1.56×10^{12}	1.046	1.52×10^{12}

In order to compare all the presented models of n_i, in Fig. 4, the various predictions of $n_{i,x}(T)$ are shown normalized relative $n_{i,Hensel}$ from Hensel.[18] The normalization by Hensel's model is necessary to compare the models over a large temperature range because the values of n_i vary across several orders of magnitude. Hensel's model was chosen for the normalization because it is the closest theoretical model to empirical data, and the empirical models do not have a wide temperature range of validity.

Regarding the proposed expressions of $n_i(T)$ in the original paper by Sproul and the work of Misiakos, the substitution of a constant C coefficient rather than $E_g^0(T)/(2k)$ in the theoretical expression (Eq. (1)) is questionable for low temperatures. The impact of a temperature-dependent E_g^0 on the value of n_i should not be ignored.

IV. DENSITY OF STATES EFFECTIVE MASSES IN THE CONDUCTION BAND AND THE VALENCE BAND

It is convenient to model the temperature dependence of m_{dc}^* and m_{dv}^* in order to easily model N_V and N_C according to the new expression of n_i. The weak temperature dependence of m_{dc}^* in contrast to m_{dv}^* allow us to consider the theoretical dependence of m_{dc}^* as well as that derived from the temperature dependence of m_l^* and m_t^*. Theoretically, m_l^* is invariant with respect to temperature[23] and its value at 4 K has been accurately measured.[18] As regards m_t^*, the model suggested by Green[2] (Eq. (17)) is in good agreement with the experimental data of Ousset[24]

$$m_l^* = 0.9163 \cdot m_0, \tag{16}$$

$$m_t^* = 0.1905 \cdot m_0 \left(\frac{E_g^0(0)}{E_g^0(T)}\right). \tag{17}$$

Thus, $\left(m_{dc}^*(T)/m_0\right)^{\frac{3}{2}}$ can be expressed for the temperature range 0 K to 400 K as presented in Eq. (18) thanks to a third order polynomial fit of $E_g^0(0)/E_g^0(T)$ from Pässler's model. The discrepancies induced by the fit are lower than 0.5% for each value in this temperature range

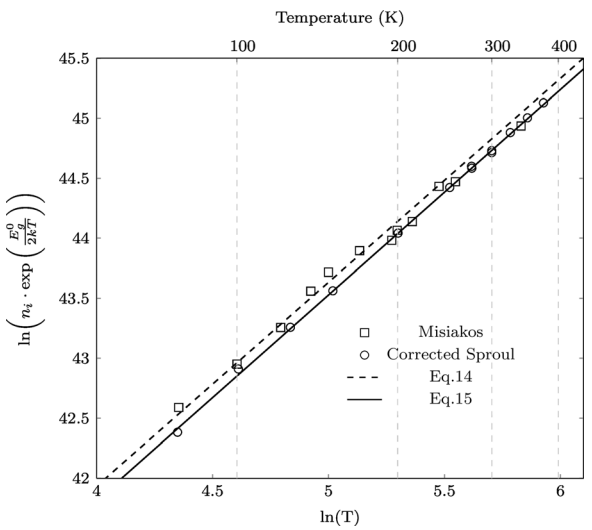

FIG. 3. $\ln\left(n_i \cdot \exp\left(\frac{E_g^0}{2kT}\right)\right)$ versus ln(T).

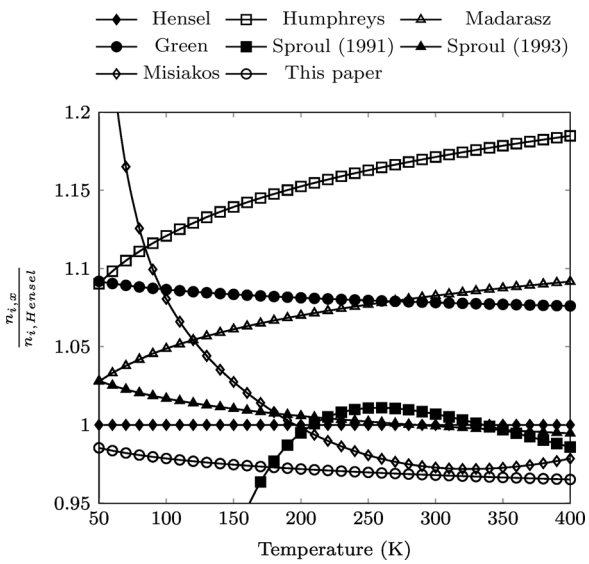

FIG. 4. $n_{i,x}$ as a function of temperature from different models normalized according to $n_{i,Hensel}$ given by Hensel.[18]

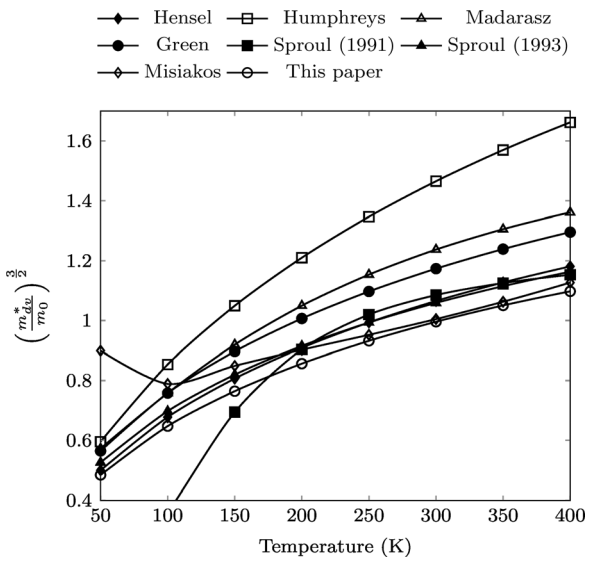

FIG. 5. $\left(\frac{m^*_{dv}}{m_0}\right)^{\frac{3}{2}}$ versus temperature extracted from different models.

$$\left(\frac{m^*_{dc}(T)}{m_0}\right)^{\frac{3}{2}} = A_c T^3 + B_c T^2 + C_c T + D_c, \qquad (18)$$

where

$$A_c = -4.609 \times 10^{-10}, \quad B_c = 6.753 \times 10^{-7},$$
$$C_c = -1.312 \times 10^{-5}, \quad D_c = 1.094.$$

In contrast to m^*_{dc}, m^*_{dv} has a high dependence on temperature, and experimental data do not support current theoretical models.[18–20] Based on Eqs. (1), (4), (5), (18), $E^0_{g,Pässler}$, and the models of n_i, it is possible to obtain an expression of $\left(m^*_{dv}(T)/m_0\right)^{\frac{3}{2}}$ according to a model of n_i and to propose a third order polynomial expression. In order to illustrate the discrepancies between the models of n_i, the temperature evolution of $\left(m^*_{dv}(T)/m_0\right)^{\frac{3}{2}}$ according to the different models of n_i is shown in Fig. 5.

The polynomial obtained with Eq. (15) is

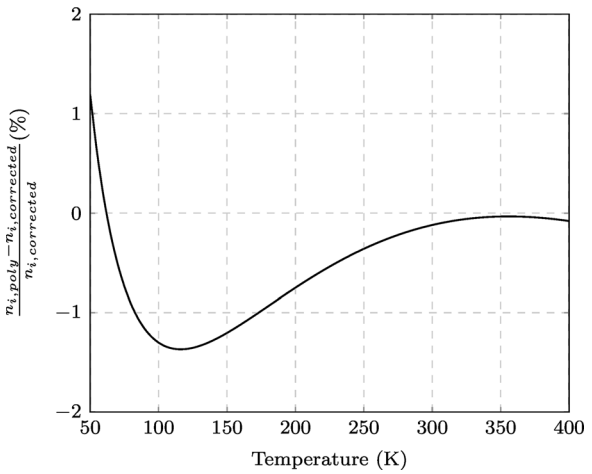

FIG. 6. Relative error of $n_{i,poly}$ as a function of temperature determined using polynomial fits of the effective masses compared to $n_{i,corrected}$ from Eq. (15).

$$\left(\frac{m^*_{dv}(T)}{m_0}\right)^{\frac{3}{2}} = A_v T^3 + B_v T^2 + C_v T + D_v, \qquad (19)$$

where

$$A_v = 2.525 \times 10^{-9}, \quad B_v = -4.689 \times 10^{-6},$$
$$C_v = 3.376 \times 10^{-3}, \quad D_v = 3.426 \times 10^{-1}.$$

In order to evaluate how the polynomials (Eqs. (18) and (19)) reproduce n_i, they are inserted in Eqs. (1), (4), and (5). The resulting expression is $n_{i,poly}$. This expression reproduces correctly $n_{i,corrected}$ from Eq. (15) as it is shown in Fig. 6 where the relative error of $n_{i,poly}$ compared to $n_{i,corrected}$ is shown as a function of temperature. The individual point discrepancies in the range 50 K to 400 K are less than 1.5%.

V. CONCLUSION

In this study, a reassessment of the temperature dependence of n_i is proposed. The impact of E^0_g on the temperature dependence of n_i has been exposed and the Pässler's model of E^0_g has been identified as the most accurate. A new expression of the temperature dependence of n_i is suggested, $n_i = 1.541 \times 10^{15} T^{1.712} \exp(-E^0_g/(2kT))$, based on Sproul's data and Schenk's model of BGN. This reassessment has served to demonstrate the convergence of Sproul's data, Misiakos' data, and Hensel's model. Finally, third order polynomials of $(m^*_{dv}/m_0)^{\frac{3}{2}}$ and $(m^*_{dc}/m_0)^{\frac{3}{2}}$ are proposed, offering a practical estimate of N_V and N_C taking into account the suggested temperature dependence of n_i. Using these polynomials to reproduce the temperature dependence of n_i provides an estimate with a precision of 1.5% for the range 50 K to 400 K.

ACKNOWLEDGMENTS

Funding for this project was provided by a grant from la Région Rhône-Alpes.

[1]J. J. Wysocki and P. Rappaport, J. Appl. Phys. **31**, 571 (1960).
[2]M. A. Green, J. Appl. Phys. **67**, 2944 (1990).
[3]A. B. Sproul and M. A. Green, J. Appl. Phys. **70**, 846 (1991).
[4]A. B. Sproul and M. A. Green, J. Appl. Phys. **73**, 1214 (1993).
[5]K. Misiakos and D. Tsamakis, J. Appl. Phys. **74**, 3293 (1993).
[6]P. P. Altermatt, A. Schenk, F. Geelhaar, and G. Heiser, J. Appl. Phys. **93**, 1598 (2003).
[7]A. Schenk, J. Appl. Phys. **84**, 3684 (1998).
[8]S. M. Sze, *Physics of Semiconductor Devices* (John Wiley, 2007).
[9]P. J. Mohr, B. N. Taylor, and D. B. Newell, Rev. Mod. Phys. **84**, 1527 (2012).
[10]G. Dresselhaus, A. Kip, and C. Kittel, Phys. Rev. **98**, 368 (1955).
[11]W. Bludau, A. Onton, and W. Heinke, J. Appl. Phys. **45**, 1846 (1974).
[12]G. G. Macfarlane, T. McLean, J. E. Quarrington, and V. Roberts, Phys. Rev. **111**, 1245 (1958).
[13]C. D. Thurmond, J. Electrochem. Soc. **122**, 1133 (1975).
[14]V. Alex, S. Finkbeiner, and J. Weber, J. Appl. Phys. **79**, 6943 (1996).
[15]Y. Varshni, Physica **34**, 149 (1967).
[16]R. Pässler, Phys. Rev. B **66**, 085201 (2002).
[17]R. Pässler, Phys. Status Solidi B **236**, 710 (2003).
[18]J. C. Hensel and G. Feher, Phys. Rev. **129**, 1041 (1963).
[19]F. L. Madarasz, J. E. Lang, and P. M. Hemeger, J. Appl. Phys. **52**, 4646 (1981).
[20]R. G. Humphreys, J. Phys. C: Solid State Phys. **14**, 2935 (1981).
[21]J. C. Hensel, H. Hasegawa, and M. Nakayama, Phys. Rev. **138**, A225 (1965).
[22]J. M. Luttinger, Phys. Rev. **102**, 1030 (1956).
[23]R. A. Stradling and V. V. Zhukov, Proc. Phys. Soc. **87**, 263 (1966).
[24]J. C. Ousset, J. Leotin, S. Askenazy, M. S. Skolnick, and R. A. Stradling, J. Phys. C: Solid State Phys. **9**, 2803 (1976).